International Journal of Science and Research (IJSR)
ISSN (Online): 2319-7064
Impact Factor (2012): 3.358

Experimental Study of Angular Dependence of Scattering Differential Cross-Sections in Double-Photon Compton Scattering Using A Scintillation Detector

Manju Bala Saddi[1], Balvir Singh Sandhu[2], Bhajan Singh[3]

[1]Mata Ganga Khalsa College for Girls, Kottan (Ludhiana)-141412, India

[2, 3]Physics Department, Punjabi University, Patiala-147002, India

Abstract: ***The doubly differential collision cross-sections of double-photon Compton process have been measured for 662 KeV incident γ-photons by using a scintillation detector. This technique avoids the use of complicated slow-fast coincidence set-up used till now for observing this higher order process. The measurements confirm that the probability of occurrence of this process is being quite small, energy spectra of the two final photons being continuous and the occurrence of this process is more pronounced when one of the two final photons is soft. The present results are in good agreement with the theory of Mandl and Skyrme. Purpose: The doubly differential collision cross-sections of two-photon Compton process have been measured for 0.662 MeV incident gamma photons. The observation are successfully carried out using a single gamma detector, a technique avoiding the use of complicated slow-fast coincidence set-up used till now for observing this higher order process. Methods and Materials: A collimated beam of 0.662 MeV gamma rays from 6.0 Ci ^{137}Cs radioactive source is made to impinge on an aluminium target. A properly shielded NaI(Tl) scintillation detector having dimensions 51mm × 51mm, placed at 50° and 70° to the incident beam, detects the scattered photons in this process. To obtain counts purely due to two-photon Compton scattering, in which one of the two final photons is emitted in the direction of the detector, the counts due to other processes are eliminated or minimized. Results: The measured values of doubly differential collision cross-section, for different energy values of one of the two final photons are of the same magnitude, but show a deviation from the corresponding values calculated from the theory within experimental errors. There are no other experimental data available for comparison with the present results. Conclusions: The agreement of the measured values of doubly differential collision cross-sections with theory is acceptable. The present measurements confirm that the probability of occurrence of this process is being quite small, energy spectra of the two final photons being continuous and the occurrence of this process is more pronounced when one of the two final photons is soft.***

Keywords: Doubly differential collision integral cross-section; energy spectra; false events and detector efficiency.

1. Introduction

The quantum electrodynamics (QED) predicts the existence of higher order double photon Compton scattering process in which the collision products are two simultaneous emitted photons and one recoil electron. Heitler and Nordheim[1] postulated the existence of this phenomenon and calculated the higher order of magnitude of the cross-section in constraints, unfavorable for experimental verification. Eliezer[2] derived an expression for the collision differential cross-section of this process in the limiting case of one hard and one soft photon only. Mandl and Skyrme[3] have provided an exact theory. The expression for collision differential cross-section derived by using S-matrix formulation of QED can be regarded as double photon Compton analog of the well-known Klein_Nishina relation for single- photon Compton scattering.

This non- linear QED process has wide scope in various fields because

1) It is a major background process in the experimental study of another QED process namely photon splitting in the fields of heavy atoms, the first experimental confirmation of which has recently been reported by Akhmadaliev et al[4].
2) It provides a mechanism of photon multiplication along with the bremsstrahlung in astrophysics.
3) Aarti et al (2004)[5] observed that for MeV incident energies the total cross-section for this process to occur is smaller by an order of magnitude as compared to that for the single-photon Compton scattering (SPCS). Thus, at the higher incident energies (where this process is more likely to occur), this effect contributes appreciably to the total scattering co-efficient.
4) Heitler and Nordheim[1](1934) have described this process as a valuable test of QED in an implicit way, although QED has been tested to a much higher accuracy.

All the experimental observations performed on double photon Compton effect till now are based on slow-fast coincidence set-up (Cavanagh[6] 1952; Bvacci[7] et al, 1956; McGie[8] et al, 1966; Sandhu[9-11] et al, 1999, 2000, 2001; Dewan[12-13] et al, 2002, 2005). In these experiments, the dimensions of both final photons are kept fixed and their coincidences are counted. Due to technical difficulties in handling of coincidence set-up and low value of intensity of double photon Compton scattering process, it needs a longer time to set good statistical results in counting rate. Carrassi and Passstore[14] (1961) proposed a method to observe double photon Compton scattering effect without the use of coincidence measurement.

So, in the present measurements, the doubly differential collision cross-sections of this process are measured at the

scattering angles of 50° and 70° to the incident beam. The measurements are carried out using a single gamma detector, a technique avoiding the use of the complicated slow-fast coincidence set-up used till now for observing this process. The energy spectrum of one of the two final photons emitted in directions of the gamma detector should be seen as a tail to the single-photon Compton line on the side of low energies.

2. Theory

Figure 1 shows the coordinate system used to describe the DPCS process.

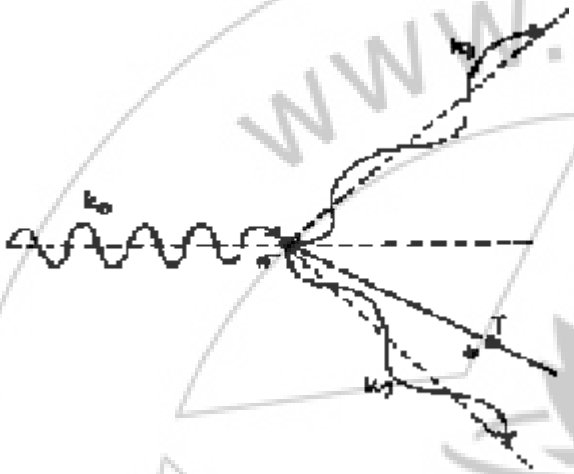

Figure 1:

The z-axis is taken to be collinear with the momentum vector of the incident photon having energy k_0. The xz-plane through z-axis contains momentum vector of one of the two final photons emitted in this process. The polar angle θ_1 defines direction of emission of this photon having energy k_1. The angles (θ_2, ϕ_2) and (θ_3, ϕ_3) define direction of emission of the other photon (having energy k_2) and recoil electron respectively. It is assumed that the electron is initially free and at rest in this reference frame.

The conservation of energy (energies being expressed in m_0c^2 units) for the above interaction gives:

$$k_0 + 1 = k_1 + k_2 + (1-\beta^2)^{-1/2} \quad (1)$$

Where $\beta = v/c$ and v is the velocity of recoil electron.
The conservation of momenta (in m_0c units) along the x, y and z-axes give

$$\text{x-component: } 0 = k_1\sin\theta_1 + k_2\sin\theta_2\cos\phi_2 + \beta(1-\beta^2)^{-1/2}\sin\theta_3\cos\phi_3 \quad (2)$$

$$\text{y-component: } 0 = k_2\sin\theta_2\sin\phi_2 + \beta(1-\beta^2)^{-1/2}\sin\theta_3\sin\phi_3 \quad (3)$$

$$\text{z-component: } k_0 = k_1\cos\theta_1 + k_2\cos\theta_2 + \beta(1-\beta^2)^{-1/2}\cos\theta_3 \quad (4)$$

The energy k_2, of one of the two final photons, in terms of k_0 (incident photon energy), k_1 (energy of the other photon) and scattering angles is given by

$$k_2 = \frac{k_0 - k_1[1 + k_0(1-\cos\theta_1)]}{1 + k_0(1-\cos\theta_2) - k_1(1-\cos\theta_{12})} \quad (5)$$

With θ_{12} being the angle between momentum vectors of the two emitted photons, and is given by

$$\cos\theta_{12} = \cos\theta_1\cos\theta_2 + \sin\theta_1\sin\theta_2\cos\phi_2 \quad (6)$$

Thus the energy k_2 (k_0; k_1, θ_1, θ_2, ϕ_2) is a function of five variables in contrast to a function of two variables k' (k_0; θ) in case of single photon Compton scattering.
Mandl and Skyrme[3] have provided an expression for the collision differential cross-section, $(d^3\sigma_D / d\Omega_1 d\Omega_2 dk_1)_{\text{collision}}$ or in short $d^3({}_e\sigma)$, for DPCS for the case in which a photon with energy in the interval k_1 and k_1+dk_1 is ejected into an element of solid angle $d\Omega_1$ in the direction θ_1, the other emitted photon being ejected into an element of solid angle $d\Omega_2$ in the direction (θ_2, ϕ_2) and its energy, k_2, is given by equation (5). Their expression for the collision differential cross-section is given by the following eqn.

$$\left(\frac{d^3\sigma_D}{d\Omega_1 d\Omega_2 dk_1}\right)_{\text{collision}} = \frac{\alpha r_0^2}{16\pi^2}\frac{k_1k_2}{k_0}\frac{X}{T_c} \quad (7)$$

Where α is the fine structure constant, r_o is the classical electron radius, and X and T_c are complicated functions of the energies and scattering angles, and are given by

$$X = -2(\eta\beta-\gamma)^2 + 4(\eta\beta-\gamma)(\eta+\beta) - 16\eta\beta + 8\gamma - 2x(\eta^2+\beta^2) + 2(\eta\beta-\gamma)x(\eta+\beta) - \frac{4x}{AB}[x^2(\delta-1) - 2\delta] + 4x(x+1)\left(\frac{1}{A}+\frac{1}{B}\right) - 4[2x + \delta(1-x)]\left(\frac{\eta}{B}+\frac{\beta}{A}\right) - 2[\eta\beta + \gamma(1-x)]\rho \quad (8)$$

and

$$T_c = 1 + k_0(1-\cos\theta_2) - k_1(1-\cos\theta_{12}) \quad (9)$$

Where η, β, ... are defined in terms of the a_i and b_i by

$$\eta = \sum_{i=1}^{3}\frac{1}{a_i},\quad \beta = \sum_{i=1}^{3}\frac{1}{b_i},\quad \gamma = \sum_{i=1}^{3}\frac{1}{a_ib_i},$$

$$A = a_1a_2a_3,\quad B = b_1b_2b_3,\quad \delta = \sum_{i=1}^{3}a_ib_i,$$

$$\rho = \sum_{i=1}^{3}\left(\frac{a_i}{b_i}+\frac{b_i}{a_i}\right),\ \text{and}\ x = \sum_{i=1}^{3}a_i = \sum_{i=1}^{3}b_i \quad (10)$$

With a_i, b_i can be written in terms of photon energies and momenta as

$$a_1 = k_1,\ b_1 = -[k_1(1+k_0-k_2) + \vec{k}_1.(-\vec{k}_0+\vec{k}_2)$$
$$a_2 = k_2,\ b_2 = -[k_2(1+k_0-k_1) + \vec{k}_2.(-\vec{k}_0+\vec{k}_1)]$$
$$a_3 = -k_0,\ b_3 = [k_0(1-k_1-k_2) + \vec{k}_0.(\vec{k}_1+\vec{k}_2)] \quad (11)$$

With $\vec{k}_0$, $\vec{k}_1$ and $\vec{k}_2$ being the momenta (in m_0c units) of the incident and two simultaneously emitted photons respectively.
On the other hand, the doubly differential collision cross-section integrated over direction of one of the two final photons, the direction of the other one being kept fixed, will provide a factor of about ten in the cross-section as an effect of the angular integration. This double differential collision cross-section can be obtained from equation (7) by the following integration.

$$\left(\frac{d^2\sigma_D}{d\Omega_1 dk_1}\right) = \int_0^{2\pi}\int_0^{\pi} d^3({}_e\sigma)\sin\theta_2 d\theta_2 d\phi_2 \quad (12)$$

The singly differentiated cross-sections of this process are of two types. One involves the integration of equation (7) over directions of both the final photons, and the other involves integration over direction of one of the two final photons and the independent final photon energy. In the first case the singly differentiated cross-sections are given by

$$\left(\frac{d\sigma_D}{dk_1}\right) = 2\pi \int_0^{2\pi}\int_0^{\pi}\int_0^{\pi} d^3({}_e\sigma)\sin\theta_1 \sin\theta_2 d\theta_1 d\theta_2 d\phi_2 \quad (13)$$

In the second case one has to select a threshold for independent final photon energy, as the collision differential cross-section exhibits infrared-divergence for either $k_1 \to o$ or $k_2 \to o$. The minimum threshold for one of the final photon energy determines the maximum threshold energy of the other photon. The singly differentiated double photon Compton cross-sections are thus provided by

$$\left(\frac{d\sigma_D}{d\Omega_1}\right) = \int_{k_1^{min}}^{k_1^{max}} \int_0^{2\pi}\int_0^{\pi} d^3({}_e\sigma)\sin\theta_2 d\theta_2 d\phi_2 dk_1 \quad (14)$$

These cross-sections can be compared with Klein-Nishina cross-section for single photon Compton scattering.

Another integration over the direction of the remaining final photon provides the total cross-section for this process to occur as a function of incident photon energy, and is thus given by

$$\sigma_D(k_0) = 2\pi \int_{k_1^{min}}^{k_1^{max}} \int_0^{2\pi}\int_0^{\pi}\int_0^{\pi} d^3({}_e\sigma)\sin\theta_1 \sin\theta_2 d\theta_1 d\theta_2 d\phi_2 dk_1 \quad (15)$$

This total cross-section can be compared with the following expression for single photon Compton scattering:

$$\sigma_S(k_0) = \frac{\pi r_0^2}{k_0}\left[\left\{1 - \frac{2(1+k_0)}{k_0^2}\right\}\ln(1+2k_0) + \frac{1}{2} + \frac{4}{k_0} - \frac{1}{2(1+2k_0)^2}\right] \quad (16)$$

The expressions for integral cross-sections are quite complicated functions of energies and directions of the emitted quanta, and their physical contents are difficult to display.

3. Experimental set-up

The experimental set-up used for the measurements of double photon Compton scattering of 661.65 keV gamma rays is shown in Figure 2. The radioactive source ^{137} Cs of strength 8.0 Ci, which emits gamma rays of energy 661.65 keV, used in the present study is placed in the cavity (having dimensions 88 mm in length and 29 mm in diameter) of the rectangular lead container of dimensions 200 mm x 160 mm x 160 mm A conical lead cork provided with cylindrical opening having aluminium walls and of diameter 35 mm and length 61 mm is fitted permanently in the container with the help of screws. In the cylindrical lead c ork an aluminium window of thickness 141.5 mg cm^{-2} (absorption of 661.65 keV gamma rays is less than 1 %) is fixed facing towards the source. A brass stopper having diameter 34.5 mm, length 62 mm and filled with lead can be inserted into the cylindrical opening to close the incident beam when required. A cylindrical beam collimator consisting of a brass pipe of internal diameter 25 mm, length 80 mm and aluminium windows of thickness 222.4 mg cm^{-2}, fixed permanently in a lead slab, which absorbs only 1.6% of 661.65 keV gamma rays. The brass collimator is connected to mercury reservoir through pipe and it can be filled with mercury or unfilled by moving the mercury reservoir up and down respectively. A conical lead collimator of length 80 mm and having diameters of 28 mm and 40 mm on the two sides reduces the effect of scattering from the edges.

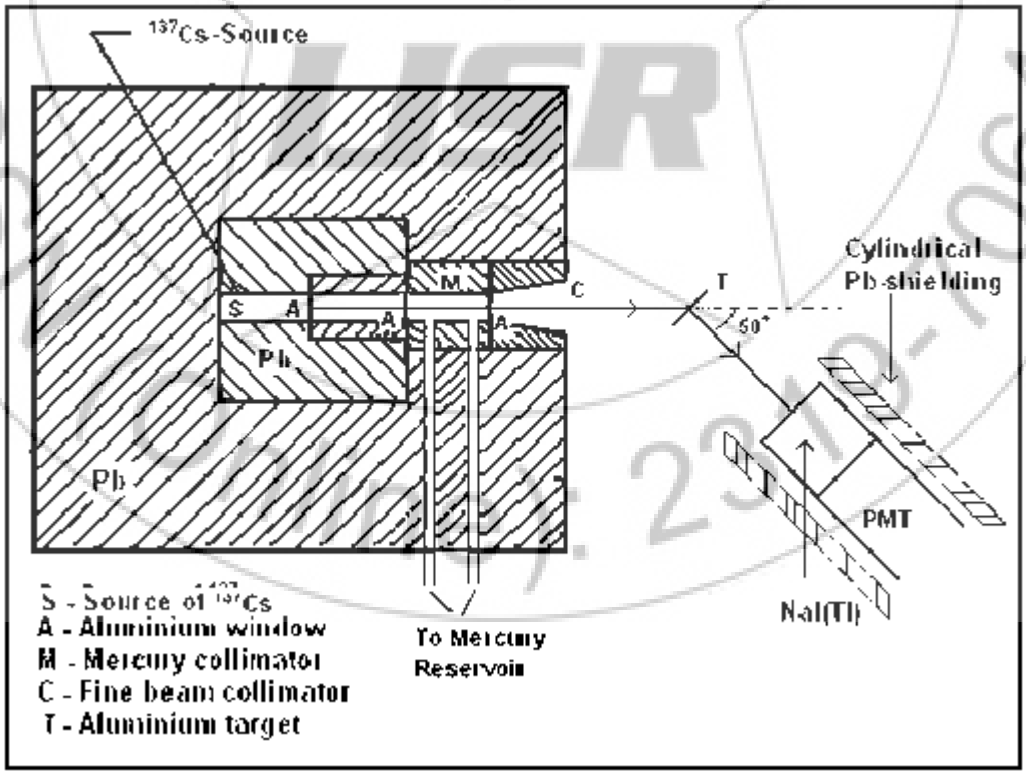

Figure 2:

The source container, mercury and conical lead collimator are placed horizontally on one side of 10 mm thick aluminium table so that the entire system is co-axial and is shielded with additional lead bricks each of dimension 160

mm x 80 mm x 40 mm on all the sides such that the entire assembly becomes rectangular in shape with dimensions of 480 mm x 320 mm x 320 mm shown in Fig. 2. In order to reduce the scattering from the table the source is placed at a height of 380 mm from the surface of the scattering table. The scattering from the walls of the room can be minimized by placing the scattering table near the window of the room. When the cylindrical beam collimator is filled with a column of mercury, the background near the system comes out upto the natural background level, it confirms the proper shielding of the radioactive source which is one of the essential requirement of present experimental measurements.

On one side of the scattering table radioactive source housing is placed and on the other side of it a scatterer holder assembly, is fixed. The scatterer holder is designed in such a way that it should cover the whole incident beam and the angular position of the γ detector can be adjusted by giving a proper orientation with respect to the incident beam and directions of the scattered gamma rays. The scatterer holder is made of aluminium frame with dimensions of 50 mm x 50 mm on which the scatterer can be easily fixed. The scatterer mount arrangement consists of brass rod of diameter 7.0 mm and of adjustable length (350 ± 50 mm) fixed to one end of a slide which moves on an aluminium disc of diameter 140 mm.

In the present study of double photon Compton scattering process, γ detector is used to detect the one of the two final photons originating from interaction of incident radiation with the target electrons. It consists of 51 mm diameter x 51 mm thickness, NaI(Tl) scintillation crystal, having 0.38 mm thick aluminium window and optically coupled to RCA-8053 photomultiplier tube. Detector is shielded by cylindrical lead shielding (140 mm in length and 27.5 mm thick) of inner diameter 60 mm. The inner side of this shielding is covered with 2 mm thick iron and 1 mm thick aluminium with iron facing towards lead to absorb the lead K X-rays emitted by lead shielding. Detector is placed on a movable arm, which can rotate around the scatterer mount on the scattering table. The distance of the detector from the centre of the scattering table can be varied upto 400 mm and height of the detector from the surface of the scattering table is adjustable from 300 mm to 500 mm. The γ detector does not face the source window directly and is placed 40 mm inside the lead shielding to prevent photons scattered from edges of the collimator from reaching the active volume of the detector. The observed count rate is not affected by the γ detector shielding and is only due to the radiation originating from the interaction of gamma rays with the target electrons reach the γ detector. In the present measurements, the distance of the scatterer from radioactive source is kept fixed (350mm), thus the solid angle subtended by the scatterer at source being 0.02 steradian. The γ detector is placed at 50° and 70° to the incident beam and at a distance of 410 mm from the scatterer. This give rise to the angular spread of ±3.6° about the median ray in the direction of the γ detector.

Energy calibration of NaI(Tl) detector is carried out by using ^{133}Ba (81 keV and 356 keV), ^{22}Na (511 keV) and ^{137}Cs (662 keV) calibration sources. The photopeak efficiency curve for the γ detector is shown in Figure 3.

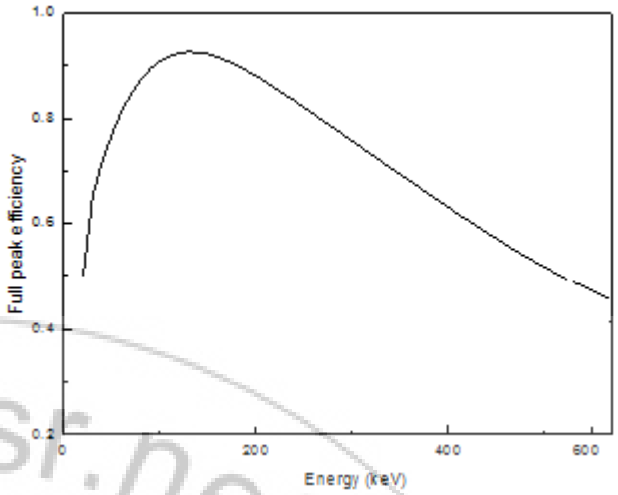

Figure 3

The curve is obtained from data for intrinsic efficiency and photofraction reported by Crouthamel (1960), and corrected for iodine escape peak (Axel, (1954); Veigele, (1973) and absorption in aluminium windows (Hubbell, 1977). The photopeak efficiency values are also measured experimentally using single energy sources of known strength of ^{203}Hg (279 keV) and ^{137}Cs (662 keV). Energy spectrum is recorded by placing the radioactive sources at the position of known activity at the scatterer position. The solid angle subtended by the detector at the centre of the source is thus the same as in the actual measurements. The distance of the NaI(Tl) detector from the source centre being large in the comparison to the aperture of the γ detector, so incident gamma beam is being normal to the detector face, and the intrinsic efficiency (ε_i) is given by

$$\varepsilon_i = 1\text{-}e^{-\mu t} \quad (17)$$

The value of the intrinsic efficiency is evaluated by knowing the values of attenuation coefficients and the detector thickness. The product of the probability of detecting a radiation falling on the detector (detection efficiency) and the fraction of radiation detected by the crystal which dissipates full energy in it (photofraction) gives the photopeak efficiency of NaI(Tl) detector for that particular incident photon energy. The experimentally measured valued of photopeak efficiency using single energy sources of ^{203}Hg and ^{137}Cs of known source strengths results to be 0.67 ± 0.03 and 0.31 ± 0.02 respectively, and are in agreement with corresponding theoretical values of 0.70 and 0.30.

4. Method of Measurement

When a gamma ray impinges on a free and stationary electron, there is a probability for the simultaneous emission of two photons along-with a recoil electron in the double photon Compton scattering process. The principle of present measurements is to detect the scattered energy spectra using a gamma ray detector placed at 50° and 70° to the incident beam. The energy spectrum of the detected photon is observed as a long tail on the lower side of the full energy peak observed in single or normal Compton scattering. The events resulting from the single-photon Compton process (scattered photon is emitted in direction of the γ detector) and double-photon Compton scattering (in which one of the

two final photons is emitted in direction of γ detector) are extracted from the recorded scattered spectra.

The number of counts registered per unit time from double photon Compton scattering events in which one of the two final photons, having energy in the interval E_1 and $E_1 + \Delta E_1$, is scattered in the direction of gamma detector and the direction of the second emitted photon being emitted into solid angle of 4π in space are given by

$$N_d = I_0 n_e t \left(\frac{d^2\sigma_D}{d\Omega_1 dE_1} \right)_{\Delta E_1} \beta_{\gamma d}\, \varepsilon_1(\Delta E_1) d\Omega_1 \quad (18)$$

Where I_0 is the incident γ flux at the scatterer; n_e is the number of electrons per unit volume of the scatterer, t is the thickness of the scatterer and $\varepsilon_1(\Delta E_1)$ is the average efficiency of the gamma detector corresponding to photon energy (in the interval E_1 and $E_1 + \Delta E_1$) of one of the two final photons resulting from double photon Compton scattering and detected by the gamma detector. $\beta_{\gamma d}$ is the self-absorption correction factor for incident and scattered radiation in double-photon Compton scattering. $d\Omega_1$ is the solid angle subtended by gamma detector at the center of the scatterer. $\left(\frac{d^2\sigma_D}{d\Omega_1 dE_1} \right)$ is the probability for double photon Compton scattering process to occur in the case when one of the two final photons carrying an energy E_1 is scattered into an element of solid angle $d\Omega_1$ and the other photons is emitted anywhere within solid angle of 4π in space.

The double photon Compton scattering cross-sections are measured relative to single photon Compton scattering cross-section, which eliminates the measurement of quantities like absolute source strength N, source scatterer solid angle Ω_0, target scatterer solid angle Ω_1, scatterer thickness t and number of electrons per unit volume of the scatterer n_e because these quantities involve uncertainty in the experimental results. The number of gamma photons scattered per second by free electrons through single photon Compton scattering events under the same experimental conditions described as above and detected by the gamma detector D is given by

$$N_S = I_0 n_e t \left(\frac{d\sigma_{KN}}{d\Omega_1} \right) \beta_{\gamma s}\, \varepsilon'(E') d\Omega_1 \quad (19)$$

Where $\varepsilon'(E')$ is the efficiency of the detector corresponding to the energy E' due to single photon Compton scattering in the direction of the detector D. $\left(\frac{d\sigma_{KN}}{d\Omega_1} \right)$ is the Klein-Nishina cross-section for single photon Compton scattering in direction of the detector D. $\beta_{\gamma s}$ is the self-absorption correction factor for incident and scattered radiation in single-photon Compton scattering Using Eqs. (18) and (19), double photon Compton scattering cross-section is given by

$$\left(\frac{d^2\sigma_D}{d\Omega_1 dE_1} \right)_{\Delta E_1} = \frac{N_d}{N_S} \left(\frac{d\sigma_{KN}}{d\Omega_1} \right) \frac{\beta_{\gamma s}}{\beta_{\gamma d}} \frac{\varepsilon'(E')}{\varepsilon_1(\Delta E_1)} \quad (20)$$

The quantities N_d and N_S are measured experimentally while efficiency of the gamma detector can be evaluated from the curve in Fig.3.

Single photon Compton cross-sections are calculated from the Klein-Nishina relations. The self absorption correction factor (in reflection geometry) is evaluated from the equation given below:

$$\beta_\gamma = \frac{1 - e^{-\left(\frac{\mu_i + \mu_e}{\cos\theta}\right)t}}{\left(\frac{\mu_i + \mu_e}{\cos\theta}\right)t} \quad (21)$$

μ_i and μ_e are the attenuation coefficients for the incident and scattered radiations respectively. The angle θ equals to 45° in symmetrical reflection geometry.

5. Sources of False Events

In addition to the events recorded in the energy spectra originate from SPCS and DPCS in which one of the two final photons is emitted in the direction of γ detector, there are many other systematic effects contributing to the count rate. These effects (processes) may arise due to the other events occurring in the scatterer, surrounding material, detector, etc. In the present measurements the main sources of these events:

1) The recoil electrons in Compton scattering and photoelectric effects may produce K X-ray by ionization during the slowing down process.
2) Bremsstrahlung produced from Compton electrons and photoelectrons.
3) The natural background, cosmic rays and weak radioactive sources present in the laboratory.
4) Single and Double photon Compton scattering events taking place from air and other surrounding materials.
5) Higher order processes like triple photon Compton scattering in which one of the final photons is emitted in the direction of γ detector.
6) Multiple Compton scattering taking place in the scatterer in which final photon escapes in the direction of γ detector.

The contribution of majority of the false events mentioned above can be minimized by proper shielding of the γ detector, selecting scatterer material of low Z atomic number and of small thickness, minimizing the surrounding material and proper biasing of the γ detector.

6. Experimental Measurements

The γ ray source is placed in the source housing described in the section 2. the γ ray spectrometer is calibrated by using standard calibration sources of different energies (^{133}Ba 81 keV and 356 keV, ^{203}Hg 279 keV, ^{22}Na 511 keV and ^{137}Cs 661.65 keV). Spectrum is recorded by placing each of the calibration sources at the scatterer position. From the recorded spectrum FWHM value corresponding to the full

energy peak is measured. Fig.4 shows the plot of FWHM as function of incident photon energy. The solid curve gives the best fit through the points corresponding to observed FWHM valued. The detector response (FWHM value) at the desired energy value can be obtained from this curve. The position and orientation of the scatterer is adjusted so that its centre coincides with the axes of source collimator and the γ detector. The measurements are then performed at the scattering angles 50° and 70° by placing aluminium scatterer of four different thicknesses in the incident γ beam.

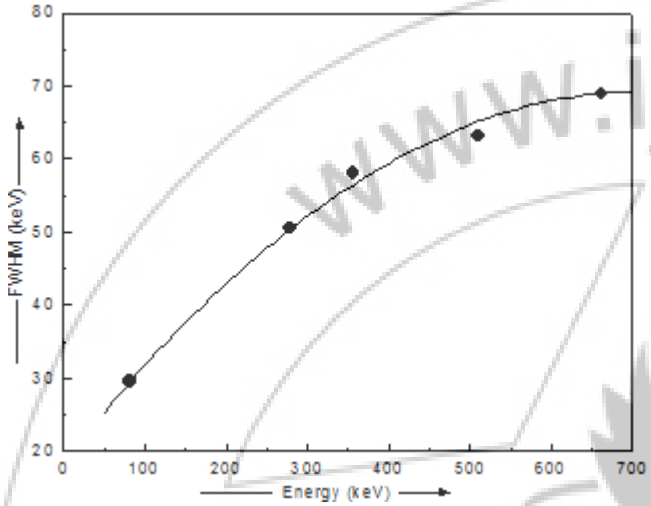

Figure 4

The following procedure is adopted for the measurements.

(i) The target-in scattered spectra are recorded for a period of 5ks by placing each of the four different aluminium scatterers (having thicknesses 40.0, 60.8, 159.6 and 236.4 mg cm^{-2}) in the primary γ ray beam.

(ii) The background is recorded after removing the aluminium target out of the primary beam to permit the registration of the events due to cosmic rays and to any other process independent of the target.

The subtraction of events recorded under condition (ii), from those condition (i) results in events originating from the interaction of primary γ rays in the aluminium scatterer. The measurements under conditions (i) and (ii) are performed in alternative time intervals with a view of avoiding errors due to possible effects of any drift in the system during measurements. As the true events resulting fro double-photon Compton scattering are few in number, the experiment is performed over a long period of time (230 ks) to achieve reasonable counting statistics. The calibration and stability of the system are checked at least once a day and adjustments are made if required.

7. Results and Discussion

In the present experiment, the scattered energy spectra are recorded for a period of 230 ks for each thickness of the scatterer and the observed spectra for the scattering angles 50° and 70° are shown in Figs. 5(a) and 6(a) respectively.

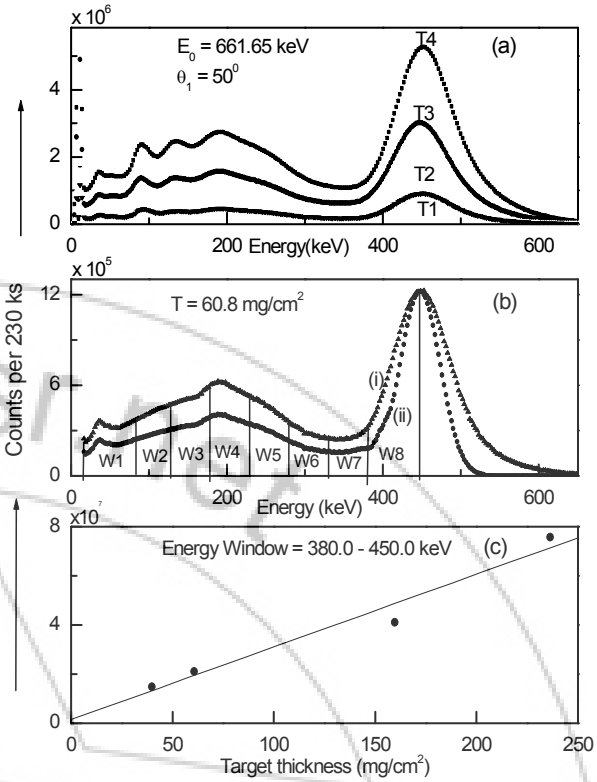

Figure 5 (a) (b) (c)

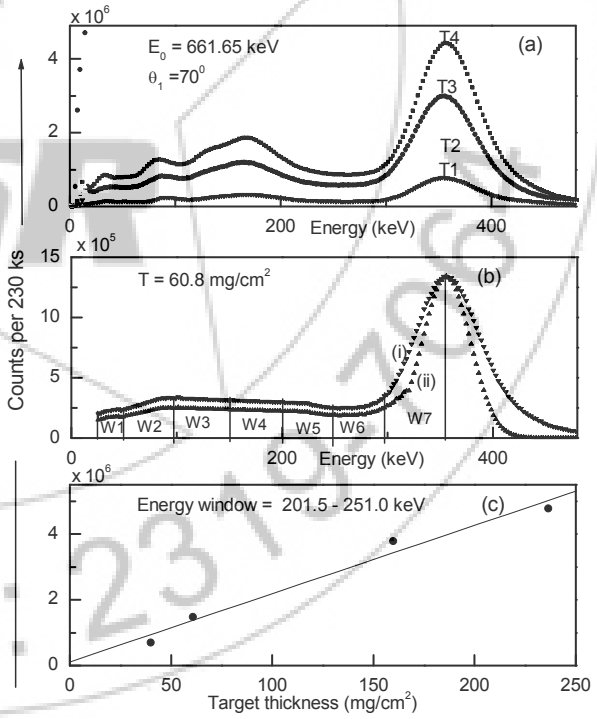

Figure 6 (a) (b) (c)

Fig. 5(a) Observed scattered spectra for 661.65 keV incident photons at scattering angle of 50° for different target thicknesses of 40.0, 60.8, 159.6 and 236.4 mg/cm^2. (b) (i) Smoothed for backscattered peak and analytically reconstructed spectrum (ii) of SPCS for target thickness of 60.8 mg/cm^2. (c) Count rate (double + bremsstrahlung +

multiple scattering)- vs- target thickness for energy window = 380.0 – 452.4 keV.

Fig. 6(a) Observed scattered spectra for 661.65 keV incident photons at scattering angle of 70° for different target thicknesses of 40.0, 60.8, 159.6 and 236.4 mg/cm^2. (b) (i) Smoothed for backscattered peak and analytically reconstructed spectrum (ii) of SPCS for target thickness of 60.8 mg/cm^2. (c) Count rate (double + bremsstrahlung + multiple scattering)- vs- target thickness for energy window = 201.5 – 251.0 keV.

It is clear that the main part of the contribution to energy spread is due to energy resolution of the γ detector. The energy spread due to detector aperture is small in comparison to intrinsic energy resolution of the γ detector. The energy spread (FWHM) due to finite target thickness shows a slight increase with target thickness but is also negligible in comparison to resolution of the γ detector. This increase in energy spread as the target thickness increase is mainly caused by multiple interactions of the incident γ photons in the target with the final photon escaping in the direction of γ detector. Some flux of the photons traveling in direction of γ detector may penetrate the NaI(Tl) crystal and is scattered back from the surface of photo-multiplier tube facing towards detector. These photons once again enter the active volume of the crystal and deposit their whole energy in the crystal and account for backscattered peak in the observed spectrum. The resulting spectrum (corrected for backscattered events) is a composite of double-photon Compton scattering (DPCS) in which one of the two final photons is emitted in the direction of detector, bremsstrahlung, multiple Compton scattering and single-photon Compton scattering (SPCS) events. Each spectrum is corrected for backscattered peak. One such typical spectrum (curve-i) for target thickness of 60.8 mg cm^{-2} is shown in Figs. 5(b) and 6(b). The events registered in the spectrum account for the following:

(i) The detection of one of the two final photons originating from DPCS process in the direction of γ detector.
(ii) The detection of the photon originating from SPCS process in the direction of γ detector.
(iii) The detection of bremsstrahlung, originating from slowing down of photoelectrons and recoil Compton electrons in the target, in direction of the detector, and
(iv) Multiple interactions taking place in the target in which the final photon escapes in the direction of γ detector.

These spectra are divided into eight different energy windows, W1 to W8 (for scattering angle 50°) and seven different energy windows, W1 to W7 (for scattering angle 70°), each having nearly 50 keV spread expect for first and last energy windows. The energy selection criterion is from channel number point of view and is then converted into energy value. The double-photon Compton collision integral cross-section is evaluated first at the scattered peak window and then in Compton continuum part. To obtain counts purely due to double-photon Compton scattering, in which one of the two final photons is emitted in the direction of γ detector, the counts due to other processes are minimized or eliminated. The major contribution among these processes is due to single-photon Compton scattering. The spectrum of SPCS is reconstructed analytically on the basis of Gaussian nature of the scattered γ ray peak using the following relation

$$y(E) = y(E_0)\exp\left\{-\frac{(E-E_0)^2}{2\sigma^2}\right\} \quad (22)$$

Where $y(E_0)$ is the number of counts at the peak energy E_0. The quantity σ is FWHM of the NaI(Tl) detector at energy E_0. The reconstructed spectrum is then normalized at the peak of experimentally observed spectrum and thus results in events purely due to the single-photon Compton scattering at the Compton scattered energy window.

A typical analytically reconstructed spectrum (curve-ii) in Figs. 5(b) & 6(b). The area under full energy peak of this analytically reconstructed spectrum provides SPCS count rate, N_s. subtraction of events under curve-ii from those under-i at the scattered energy window (W8 in Fig. 5(b) & at the scattered energy window W7 in Fig. 6(b) indicate upper limit of the energy interval, while the counts are considered for lower and upper parts of the inelastically scattered peak) results in double-photon Compton scattering, bremsstrahlung and multiple Compton events. An experimental approach, suggested by Cavanagh (1952), is used to eliminate the bremsstrahlung and multiple-scattering events. The double-photon Compton count rate varies linearly and bremsstrahlung count rate quadratically with target thickness. The dependence of count rate of multiple-Compton will be higher power in scatterer thickness. The targets used in present measurements are of small thickness, so the probability for multiple interactions taking place in the target, in which the final photon escapes in the direction of the γ detector, is negligible. A plot of counting rate (subtracted for single-photon Compton events) per unit target-thickness versus thickness would be a straight line of slope zero if target related background is negligible and a straight line of positive slope for significant bremsstrahlung background. The plot of residual counts per unit thickness versus thickness is in Figs. 5(c) & 6(c). The extrapolation of the linear curve to unit thickness provides the counts purely due to double-photon Compton scattering in which one of the two final photons is emitted in direction of the detector. The bremsstrahlung amounts on the average to about 5.4% of DPCS count rate for 60.8 mg cm^{-2} target thickness. The experimental measured values of count rates originating purely from DPCS, in which one of the two final photons is emitted in direction of the detector, for different selected energy windows are given in column 3 of Table 1 & 2. The column 6 of both tables 1&2 provides the numerical values of the ratio $\varepsilon'(E')/\varepsilon(\Delta E_1)$. The quantity, $\varepsilon'(E')$, is photopeak efficiency of the γ detector corresponding to energy E' due to single-photon Compton scattering in direction of γ detector. The quantity, $\varepsilon(\Delta E_1)$, is photopeak efficiency of the γ detector corresponding to photon energy $E_1 + \Delta E_1/2$ (average energy of the span ranging from E_1 to $E_1 + \Delta E_1$) of one of the two final photons resulting from DPCS in the direction of the γ detector.

Table 1 *
Experimental measured values of collision integral cross-section of double-photon Compton scattering angle of 50° for 661.65 keV incident γ photons

Table 2 **
Experimental measured values of collision integral cross-section of double-photon Compton scattering angle of 70° for 0.662 MeV incident γ photons

In the present measurements at scattering angles of 50° and 70°, the values of $E^{'}$ are 452.4 keV and 357.3 keV respectively and corresponding photopeak efficiency values from the curve in Fig. 3. The value of $\varepsilon_1(\Delta E_1)$ for different energy windows, W1 to W8 (for scattering angle 50°) and W1 to W7 (for scattering angle 70°), are also obtained from curve in Fig. 3 for each of the energy window. The obtained numerical value foe ratio $\varepsilon^{'}(E^{'})/\varepsilon(\Delta E_1)$ is quoted in column 6 of tables 1& 2. The column 7 of tables provides the experimental measured values of Collision Integral cross-section for different selected energy windows at scattering angles of 50° and 70° for 661.65 keV incident photons. Column 8 of the tables 1 &2 gives the corresponding values calculated from theory (Mandl and Skyrme, 1952; Sharma et al., 2004) for the same energy windows and direction of emission of one of the two final photons. The errors quoted in count rates and experimentally measured values of Collision Integral cross-section represent statistical uncertainties only.

An overall error of 6 – 18% is estimated in the present measurements and is caused by uncertainties in count rated due to double photon and single photon Compton scattering events, detector efficiencies, target thickness and self-absorption in the scatterer. The major contribution to the error is caused by statistical uncertainties in the count rate due to double-photon Compton scattering. This uncertainty is small when one of the two final photons is soft.

Table 3: Error involved in measurement of various quantities

Quantity	Nature of uncertainty	Uncertainty (%)
Measurement of N_d	Statistical	0.5 – 16.0%
Measurement of N_s	Statistical	<1%
Scatterer thickness	Systematic	<1.5%
Detector efficiency	Systematic	5%
Solid angle	Systematic	1%
Self absorption correction factor β	Systematic	<1%

The error involved in measurement of various quantities along with the nature of uncertainties is given in Table 3. The experimentally measured value of singly-differential collision integral cross-section of this process at scattering angles 50° and 70° , $\left(\frac{d\sigma_D}{d\Omega_1}\right)_{E_1 \geq 18.8 keV}$, $\left(\frac{d\sigma_D}{d\Omega_1}\right)_{E_1 \geq 21.2 keV}$, for 0.662 MeV incident γ photons comes to be (3.84 ± 0.07) × 10^{-28} cm^2/sr and (2.51 ± 0.05) × 10^{-28} cm^2/sr respectively. The corresponding values of singly-differential collision integral cross-section calculated from theory (Sharma et al., 2004) for the same lower energy limit of one of the two final photons being 3.10 × 10^{-28} cm^2/sr and 2.40 × 10^{-28} cm^2/sr.

$$\left[\left(\frac{d^2\sigma^{th}}{d\Omega_1 dE_1}\right)_{\Delta E_1}\right]_{av} = \frac{1}{\Omega_1}\int_{\Omega_1}\left(\frac{d^2\sigma^{th}}{d\Omega_1 dE_1}\right)_{\Delta E_1} d\Omega_1 \quad (23)$$

Where Ω_1 is solid angle subtended by ϒ detector at center of the scatterer. The maximum deviation of the average cross-section values from the unaveraged one is found to be less than 1%. The measured values of collision cross-section for different independent energy levels of one of the two final photons are although of same magnitude but show deviation from the corresponding values calculated from theory. The major contribution to observed counts for each energy window for both scattering angles being due to single-photon Compton scattering. On the basis of Gaussian nature of scattered gamma ray peak, the spectra for these events are reconstructed analytically. It is uncertain to state upto what fraction detector volume contributes to full or partial absorption of the photon energy incident on it, and may be the possible reason for these deviations.

The present measurements are first of its kind and probability of occurrence of this process is quite small. So, in view of the nature and order of deviations, the agreement of the measured values with theory is acceptable. There is no other data for comparison with the present results of double-photon Compton collision integral cross-section. Our understanding of the process is certainly incomplete and requires more experimental data at other scattering angles and higher photon energies to support the currently acceptable theory of this process.

References

[1] W. HEITLER and L. NORDHEIM, *Physica* 1 (1934) 1059.
[2] C. J. ELIEZER, *Proc. Roy. Soc.* (London) A187 (1946) 197.
[3] F. MANDL and T.H.R. SKYRME, *Proc. R. Soc. London Ser.* A **215,** 497 (1952).
[4] Sh Zh AKHMADALIEV et al., *Phys. Rev. Lett.* **89,** 061802 (2002).
[5] AARTI SHARMA, M. B. SADDI, B. SINGH and B.S. SANDHU, Nucl. Sci. & Engg. **148,** 445 (2004).
[6] P.E. CAVANAGH, *Phys. Rev.* 87 (1952) 1131.
[7] A. BRACCI, C. COCEVA, L. COLLI and R.DUGNAM LONATI, *Nuovo Cimento* 3 (1956) 203.
[8] M.R. McGIE, F.P. BRADY and W.J. KNOX, *Phys. Rev.* **152,** 1190 (1966).
[9] B.S. SANDHU, R. DEWAN, B. SINGH and B.S. GHUMMAN, Phys. Rev. **A 60,** 4600 (1999).
[10] B.S. SANDHU, R. DEWAN, M.B. SADDI, B. SINGH and B.S. GHUMMAN, *Nucl. Inst. & Meth.* B168 (2000) 329.
[11] B.S. SANDHU, M.B. SADDI, B. SINGH and B.S. GHUMMAN, *J. Phys. Soc. Jpn*. 70 (2001) 101.
[12] R. DEWAN, M.B. SADDI, B.S. SANDHU, B. SINGH and B.S. GHUMMAN *Nucl. Sci. & Engg.* 141 (2002) 165.

[13] R. DEWAN, M.B. SADDI, B.S. SANDHU, B. SINGH and B.S. GHUMMAN *Annals of Nuclear Energy* 32 (2005) 1008-102228.
[14] M. CARRASSI and G. PASSATORE, *IL Nuovo Cimento* 22 (1961) 1316.

Author Profile

I, M.B. Saddi received M.Sc. & Ph. D degrees from Punjabi University Patiala (India) during 1997 & 2004 respectively. My area of research is Radiation Physics and my main work done on Energy, Intensity and angular distribution of Double photon Compton Scattering of Gamma Rays. Presently working as Assistant Professor at MGK College for Girls, Kottan (Punjab).

***Table 1**

Energy Window	ΔE_1 (in keV)	N_d (per ksec)	N_s (per ksec)	$\frac{\beta_{\gamma s}}{\beta_{\gamma d}}$	$\frac{\varepsilon'(E')}{\varepsilon(\Delta E_1)}$	Collision Integral cross-section x 10^{-29} (cm^2/sr)	
						Experimental	Theory
W1	18.8 - 81.3	2950.31 ± 18.96	730947.83 ± 56.37	1.024	0.57	6.820 ± 0.044	6.027
W2	81.3 - 130.8	1414.77 ± 53.22		1.007	0.51	2.860 ± 0.107	1.663
W3	130.8-180.3	1435.47 ± 53.74		1.005	0.52	2.974 ± 0.111	1.043
W4	180.3-232.1	308.15 ± 64.55		1.003	0.57	0.693 ± 0.013	0.769
W5	232.1-281.6	227.85 ± 64.10		1.002	0.63	0.569 ± 0.014	0.641
W6	281.6-331.1	147.17 ± 63.64		1.001	0.70	0.411 ± 0.016	0.710
W7	331.1-380.0	931.68 ± 52.43		1.001	0.79	2.922 ± 0.164	1.084
W8	380.0-452.4	5799.69 ± 59.72		1.000	0.92	21.140 ± 0.217	19.060

****Table 2**

Energy Window	ΔE_1 (in keV)	N_d (per ksec)	N_s (per ksec)	$\frac{\beta_{\gamma s}}{\beta_{\gamma d}}$	$\frac{\varepsilon'(E')}{\varepsilon(\Delta E_1)}$	Collision Integral cross-section x 10^{-29} (cm^2/sr)	
						Experimental	Theory
W1	21.2 - 50.7	441.04 ± 8.64	589013.70 ± 50.61	1.090	0.83	1.182 ± 0.023	2.744
W2	50.7 - 100.2	935.97 ± 12.80		1.011	0.66	1.848 ± 0.025	1.90
W3	100.2 - 152.0	938.10 ± 63.04		1.005	0.64	1.785 ± 0.120	1.030
W4	152.0 - 201.5	296.90 ± 47.98		1.003	0.67	0.595 ± 0.096	0.687
W5	201.5 - 251.0	362.32 ± 12.10		1.002	0.74	0.797 ± 0.026	0.679
W6	251.0 - 300.0	854.04 ± 11.92		1.001	0.82	2.090 ± 0.030	1.103
W7	300.0 - 357.3	6038.64 ± 59.88		1.000	0.94	16.820 ± 0.166	15.820